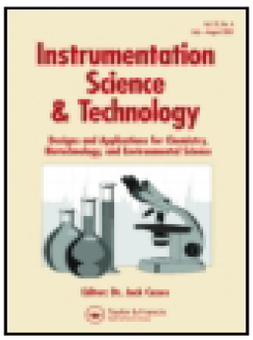

Instrumentation Science & Technology

ISSN: 1073-9149 (Print) 1525-6030 (Online) Journal homepage: http://www.tandfonline.com/loi/list20

High-sensitivity and spatial resolution transient magnetic and electric field probes for transcranial magnetic stimulator characterizations

Qinglei Meng, Michael Daugherty, Prashil Patel, Sudhir Trivedi, Xiaoming Du, Elliot Hong & Fow-Sen Choa

To cite this article: Qinglei Meng, Michael Daugherty, Prashil Patel, Sudhir Trivedi, Xiaoming Du, Elliot Hong & Fow-Sen Choa (2017): High-sensitivity and spatial resolution transient magnetic and electric field probes for transcranial magnetic stimulator characterizations, Instrumentation Science & Technology, DOI: 10.1080/10739149.2017.1401547

To link to this article: https://doi.org/10.1080/10739149.2017.1401547

INSTRUMENTATION SCIENCE AND TECHNOLOGY
https://doi.org/10.1080/10739149.2017.1401547

Taylor & Francis
Taylor & Francis Group

High-sensitivity and spatial resolution transient magnetic and electric field probes for transcranial magnetic stimulator characterizations

Qinglei Meng[a], Michael Daugherty[a], Prashil Patel[b], Sudhir Trivedi[b], Xiaoming Du[c], Elliot Hong[c], and Fow-Sen Choa[a]

[a]Department of Computer Science and Electrical Engineering, University of Maryland Baltimore County, Baltimore, MD, USA; [b]Brimrose Corp, Hunt Valley Loveton Center, Sparks, MD, USA; [c]Department of Psychiatry, University of Maryland School of Medicine and Maryland Psychiatric Research Center, Baltimore, MD, USA

ABSTRACT

Transcranial magnetic stimulation (TMS) is widely used for noninvasive brain stimulation. However, existing TMS tools cannot deliver targeted neural stimulation to deep brain regions, even though many important neurological disorders originate from there. To design TMS tools capable of delivering deep and focused stimulation, we have developed both electric and magnetic field probes to evaluate and improve new designs and calibrate products. Previous works related to magnetic field measurement had no detailed description of probe design or optimization. In this work, we demonstrated a magnetic field probe made of a cylindrical inductor and an electrical field probe modified from Rogowski coil structure. Both have much smaller size and higher directivity than commercial dipole probes. Using probe, we can calibrate and monitor any new types of TMS coil or array design and verify measured results with the other probe. We mathematically analyze their characteristics and performance and obtained a two-dimensional vector plot of the induced electric field, which matched the measured results from the second type of probe. A commercial circular coil and a figure-8 coil, with relatively complex vector field distribution, were used as examples to demonstrate the high-resolution and accurate measurement capability of our probes.

KEYWORDS

Electric field sensing; probes; transcranial magnetic stimulation

Introduction

Transcranial magnetic stimulation (TMS) technology is one of the highly used stimulation tools for diagnosis and treatment of neurological and psychiatric disorders. It takes the advantage of magnetic field's penetration depth into scalp, skull, and brain tissues, since none of these materials are ferromagnetic materials. Nerve tissues are stimulated by the induced electric field, which is generated by a time-varying magnetic field surrounding the TMS coils.

CONTACT Qinglei Meng meng2@umbc.edu Department of Computer Science and Electrical Engineering, University of Maryland Baltimore County, 1000 Hilltop Circle, Baltimore, MD 21250, USA.
Color versions of one or more of the figures in the article can be found online at www.tandfonline.com/list.

Through neural plasticity, the stimulated regions can undergo physiological changes and achieve medical effects.[1] Physiological effects of nerve systems depend on parameters of stimulation, such as repetition rate,[2] intensity, interval, duration, stimulated position, and direction.[3] It is important and necessary to be able to detect the induced electric field distribution surrounding the TMS coil to map the excitation areas and achieve targeted stimulations. Early researches on induced electric field measurements included two main methods, one of which was to use probes to directly detect current, so the probes replaced a volume of brain tissue with an equivalent conductive path.[4] Larsen and Sances' group used this kind of method and measured induced current from time-varying magnetic field inside tissue.[5–7] Their results demonstrated that the method was able to improve measurement accuracy in media with low conductivity. However, the prerequirement is that they will need very low contact impedance between probe and tissue. Furthermore, one disadvantage is that placing probes may cause tissue displacement.

The second approach to measure induced electric field is to build up small elements of dipole. Hart and Wood[8] showed that much smaller displacement of tissue would be achieved in field measurement using dipole probes. They could also significantly improve the measurement sensitivity under low-frequency TMS driving pulses. However, their dipole probes were easily interfered by electric and magnetic fields in the environment. Some recent studies reported similar results. Salinas, Lancaster, and Fox used wire tips (open circuit) together with wire loops (short circuit) to scan TMS with different shapes and achieved vector plots of induced electric field.[9,10] Lin and Wang in 2011 designed a high-dynamic range electric field senor based on domain inverted electro-optic (E-O) polymer Y-fed directional coupler for electromagnetic pulse detection.[11] The sensor they designed detected electric field between 16.7 V/m and 750 kV/m and a large dynamic range of power from 1.04 W/m^2 to 2.09×10^9 W/m^2.

Dolde and Fedder[12] detected three-dimensional induced electric field intensity with the application of quantum metrology technique, using a single nitrogen-vacancy defect center spin in diamond. Besides these types of probes and measurement principles, researchers were also working toward the goal of sensor miniaturization and integration as well as medical application. Densmore et al.[13] designed a silicon-on-insulator (SOI) photonic wire field sensor with high sensitivity. The sensor is a type of thin SOI waveguide, and a highly effective index change, of 0.31 per refractive index unit in solution, was achieved.

Another successful development of integrated electric field sensor was completed by Zeng et al.,[14] and their electrical dipole was only 60 μm but was used to measure the field in waveguide. Early in 2004, Shinawa and Fukumoto reported a near-field sensing transceiver for intrabody medium.[15]

The transceiver was composed of an electric field sensor implemented with an electro-optic crystal and laser. The electric field sensor was still a dipole structure, but different from other dipole-type probes, they used conductive pad as the electrodes so that the dipole was functioning as a capacitor.

However, researchers have not developed probes for transient electric field sensing with both high sensitivity and minimized size, for the study of electric or magnetic pulse generating medical equipment, such as TMS. In our study, we developed two types of probes for transient field measurement and built a TMS testing system for both figure-8 coil and circular coil driven by a pulse-generating circuit. The sensitivity of the probes benefited from magnetic cores in these probes' wiring and different from measurements in previous studies. So by measuring the same field intensity, our probe could induce much higher voltage at the output to significantly improve its sensitivity. Clean magnetic and electric field signals were detectable without the help of amplifiers, which may induce noise and/or nonlinear characteristic to probes. Furthermore, our probe designs had simplified structures and no microfabrication processes were required, so that the cost of the probes' manufacture would be much lower than most of the probes designed in previous studies.

In our measurements, both magnetic field and induced electric field were measured in the space under the figure-8 TMS stimulator. Data were recorded along the x- and y-axes to obtain two-dimensional field vectors. Induced electric field vectors were plotted within two planes that were in parallel with the downside surface of TMS stimulator to present field distribution in two-dimensional.

Methods

Different probe structures and measurement theory

In our experiments, transient magnetic field and/or induced electric field are generated from a commercial figure-8 shaped TMS coil (Magstim, D70 mm). Two types of probes were used in this study: a cylindrical inductor probe to estimate both electric and magnetic fields and a circular wire-wrapped electric field probe modified from Rogowski coil structure to measure the induced electric field. Both probes were connected to the oscilloscope by coaxial cables. The wiring near the TMS coil was twisted and shielded by a 5-mm-thick layer of aluminum foil.

Figure 1a shows a cylindrical inductor type of probe. It is capable of sensing the magnetic field changing rate (dB/dt) and converting it to a circulated electric field as well as presented the field as probe terminal voltages following Faraday's law.[16] The magnetic probe shares a similar principle as search coils but with a significantly improved sensitivity due to the increased number of coil turns and the additional magnetic core. In our study, we used 42

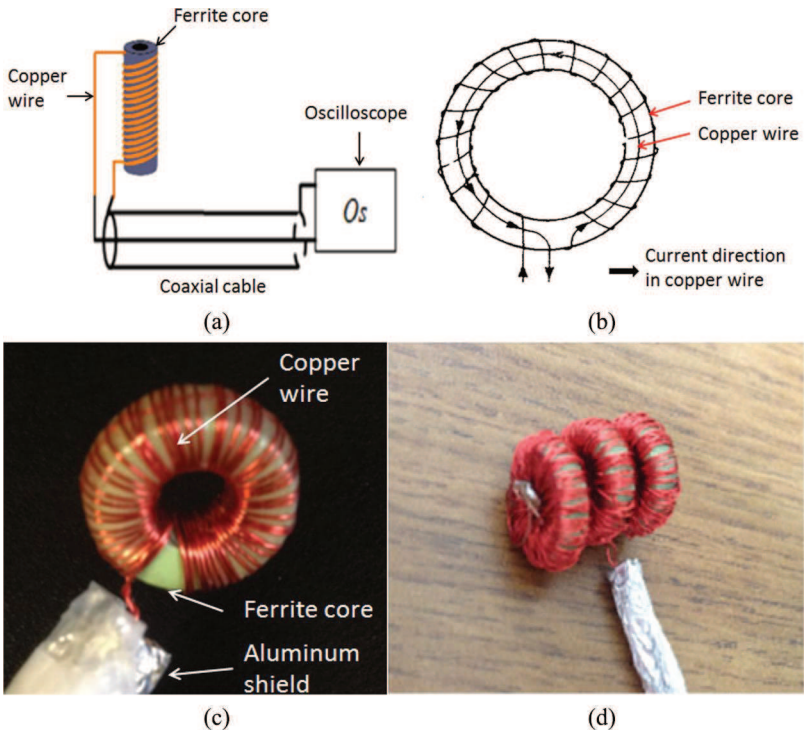

Figure 1. (a) Structure of cylindrical inductor probe; (b) structure of Rogowski coil; (c) electric field probe with one magnetic core (after the electrical wire wraps and covers the magnetic core surface, the wire routes back to the starting terminal through inside the circular coil similar to Rogowski coil, so that the signal is purely generated by electric field); (d). Electric field probe with three magnetic cores used in this study. All magnetic cores are made of iron oxide ferrite and are not conductive electrically.

American wire gauge (AWG) copper wires to wrap 1000 turns on a magnetic cylindrical core with the size of 4 mm in diameter and about 5 mm in height. The inductance of the probe was measured to be 10 mH. With magnetic probe located in a time-varying magnetic field, a potential difference can be generated according to Faraday's law. The electromotive force (known as the EMF) between the two terminals can be expressed as:

$$\Delta V = -n \times \frac{\mathrm{d}}{\mathrm{d}t} \int \int \vec{B} \cdot \mathrm{d}\vec{S} \tag{1}$$

where n is the number of copper wire turns, S is the area of the cylindrical top-down side surface, and B is magnetic intensity component that is perpendicular to S and inside the inductor. It equals to the product of μ_r and B_0, where μ_r is the permeability of probe core material and B_0 is the magnetic intensity in the air. Assuming that the magnetic field intensity is uniformly across S, Equation (1) can be rewritten as:

$$\Delta V = -n \times S \times \mathrm{d}B/\mathrm{d}t \tag{2}$$

Considering that induced electric field is mainly distributed in two-dimensional planes which are in parallel with the coil surface within the space not too far from the coil, and field intensity decay follows $1/r^2$ relation (r is the distance to coil surface), from Maxwell equations, it can also be derived that induced electric field distribution can be roughly estimated by the data collected from the cylindrical probe using the following two expressions:

$$\mathrm{E}x \propto \mathrm{d}By/\mathrm{d}t \tag{3}$$

$$\mathrm{E}y \propto \mathrm{d}Bx/\mathrm{d}t \tag{4}$$

The structure of the electric field probe is shown in Figure 1c, d, where three (not limited to 3) magnetic rings, made of nonconductive iron oxide ferrite, are stacked and their electrical wire (30 AWG copper wire) terminals are serially connected to achieve better directivity for vector field measurements. The inner and outer diameters of each magnetic ring are 6 and 11 mm, respectively, and its thickness is 4 mm. It also produces higher voltage output with enhanced sensitivity. On each magnetic ring, after the electrical wire wraps and covers the magnetic core surface, the wire routes back to the starting terminal through inside the circular coil similar to Rogowski coil,[17] so that the effect of magnetic flux passing through the ring center can be cancelled out and only the electric field that is passing through the ring center will be sensed.

Commercial eddy current probes based on Rogowski coil always have large diameters that range from several centimeters to over 10 cm. It does not provide good directivity and neither good spatial resolution. To overcome this issue, we fabricated probes based on ferrite rings with a radius of only 5 mm. With much smaller sized probe, both high spatial resolution and high field measurement sensitivity could be achieved. However, the small size of ferrite ring holes limited the number of wiring turns, which also indicates that the sensitivity was limited. To further increase the sensitivity, multiple ferrite rings could be connected in series and packaged together. As a result, the three-ring probe has already achieved very high sensitivity and no electronic amplifier is needed for measurement. According to Maxwell equations, the magnetic field flux generated in the magnetic rings can be estimated by:

$$\oint \vec{H} \cdot \mathrm{d}\vec{l} = \int \int \left(\vec{J} + \frac{\partial \vec{D}}{\partial t} \right) \cdot \mathrm{d}\vec{S} \tag{5}$$

If the measurement is taken in the air, the current density, J, is zero, and considering linear materials for electric and magnetic fields,

$$\begin{aligned} \vec{B} &= \mu \times \vec{H}, \\ \vec{D} &= \varepsilon \times \vec{E}. \end{aligned} \tag{6}$$

So with the assumption that E and B are uniformly distributed within the magnetic ring, B can be solved from the integral equation

$$B = \frac{\mu\varepsilon}{2} r \times \frac{\mathrm{d}E}{\mathrm{d}t} \tag{7}$$

where r is the radius of the magnetic ring. As a result, by applying Equation (2) again, the voltage sensed by the probe is expressed as:

$$V = -\frac{nAr\mu\varepsilon}{2} \times \frac{\mathrm{d}^2E}{\mathrm{d}t^2} \tag{8}$$

where A is the area surrounded by one copper wire turn wrapping the magnetic ring.

Experimental setup

A commercial figure-8 TMS coil (Magstim, D 70 mm) and a circular coil (Magstim, Single 90-mm remote control coil) were used to generate transient fields. Figure 2 shows the top-down view and the defined coordinates of the system for measurements and plots. The original point of this coordinate system was at the center of the figure-8 coil and circular coil right their downside surface. For the figure-8 coil, the outer diameter of each side coil was about 8 cm and the inner diameter was 4 cm; and the inner and outer diameters of the circular coils were 6 and 12 cm, respectively. For transient measurement, the driving pulse train signal was provided from a function generator with 100 μs pulse width and 300 Hz repetition rate. The driving signal was able to provide over 10 V and 100 A outputs.

The figure-8 and circular TMS coils were driven by a low-voltage source for high-sensitivity probes' development. However, the power delivered to this stimulator was not high enough to generate detectable eddy current in brain phantom. So to demonstrate the equivalency of measurement in the air and

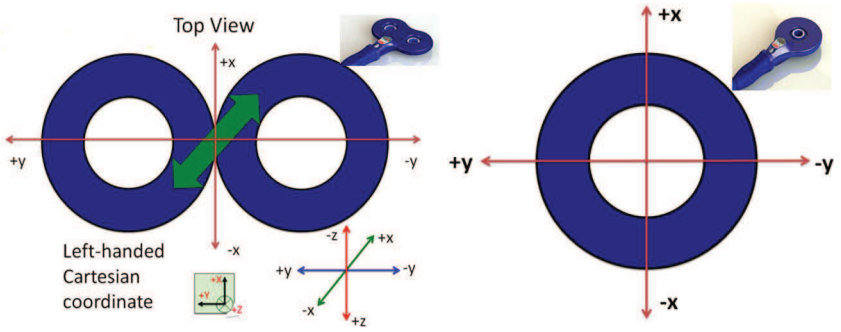

Figure 2. Figure-8 and circular TMS coils' top view and measurement coordinates. *Note*: TMS, Transcranial magnetic stimulation.

brain phantom using the inductor probe and the electric field probe modified, it was necessary to drive stimulator to generate tesla-level magnetic field. We developed a pair of smaller size circular coils for animals. The main structure and poles were made from electrical transformer.

This design in Figure 3 included two advantages: First, the magnetic material pole enhanced the magnetic field intensity; second, the pair of coils' structure rerouted magnetic flux lines so that they could not diverge quickly after they got outside the magnetic pole. The magnetic frame also restricted magnetic field and helped to achieve deeper brain stimulation. Either up or downside coil contained 1000 turns but not wrapped in series due to the required range of the overall inductance of the stimulator. Each coil was wrapped 20 turns by litz wires that contained 50 pieces of 30 AWG copper wires. However, before wrapping, litz wires were untwisted and it significantly reduced the overall inductance to the range of 10–20 μH. The stimulator was driven by an insulated gate bipolar transistor (IGBT)-controlled circuit, in

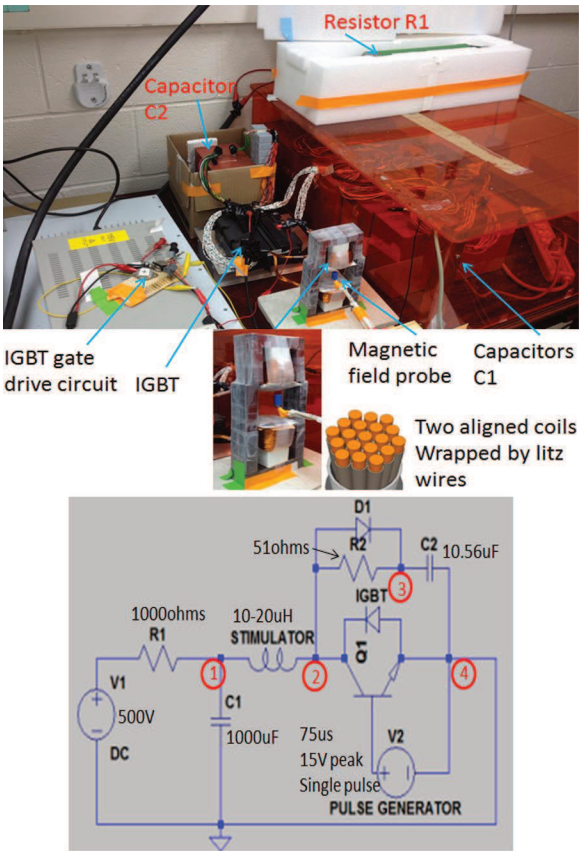

Figure 3. Animal TMS stimulator for induced electric field measurements under high magnetic field using different types of probes in both air and artificial CSF and its drive circuit. *Note*: TMS, Transcranial magnetic stimulation.

which the IGBT-controlled current pulse excitation to the stimulator (current from node 1 to node 2). The main power source was a 1000-μF capacitor (C1) charged by a high-power DC voltage supply. IGBT was protected by a snubber circuit (from node 2 to node 4 through node 3) comprised of a diode (D1), a resistor (R2), and another high-voltage capacitor (C2).

Results and discussion

Transient field measurement in the air

Figure 4 shows an example of the measured curl E signals in oscilloscope. When the driving pulse signal is applied to the TMS coil, it starts to charge the coil. The magnetic field generated by TMS stimulator is rising with a fast speed, which is picked up by the inductor probe and shows a sharp rising edge in the green trace. When the voltage on nodes 1 and 2 increased to the flat top region, the charging current from node 1 to 2 is slowing down and the dB/dt picked up by the probe shows a decreasing trace. Before the TMS coil current reached a constant, which supposed to produce zero voltage in the probe, the driving pulse turned off. Magnetic field in the TMS coil starts to discharge, which generates a negative polarity signal in the probe output with a sharp falling edge. When the discharging process gradually decreases, the inductor output starts to rise from negative value back to zero. Eventually when the current in the TMS coil became a constant, the inductor output becomes zero.

Since these probes are not able to provide absolute value of field intensity, we calibrated them with commercial TMS, for which the field intensity was

Figure 4. Example screenshot of oscilloscope for electric field sensing The yellow trace is the input pulse sent to the IGBT gate and the pink trace is the driving circuit output, namely, the voltage on nodes 1 and 2. A diode is used at circuit output to block the kickback signals from the inductor of the TMS stimulator. The green curve shows the electric signal detected by the 10 mH inductor probe. *Note*: IGBT, insulated gate bipolar transistor; TMS, Transcranial magnetic stimulation.

known at various power percentages. Figure 5a, b shows the calibration curves of electric field probe and cylindrical inductor magnetic field probe, respectively. Both probes have good measurement linearity with full output range of the commercial TMS systems, for which we know as users that about 60% of their output power can reach motor evoked potential threshold in human. It is possible by further increasing the TMS power way over 100%, the iron oxide core used in the cylindrical inductor probe may reach magnetic

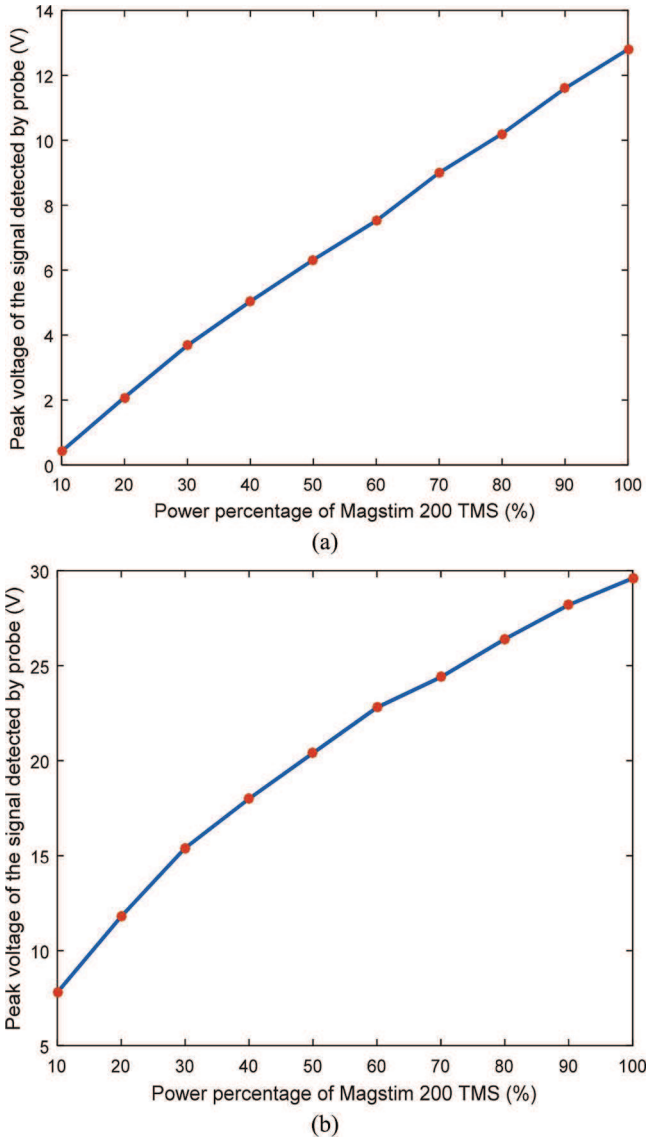

Figure 5. Calibration curves of electric field probe (a) modified from Rogowski coil and (b) cylindrical inductor magnetic field probe using the Magstim 200 TMS. *Note*: TMS, Transcranial magnetic stimulation.

saturation. In such a case, a diluted iron oxide core may need to be used to obtain good linearity at the cost of sensitivity.

Figure 6a, b shows three-dimensional plots of the x and y component amplitudes of electric field vectors with polarity for the figure-8 coil. For the electric field x component amplitude, strongest field intensity is always detected at the center of the figure-8 shaped stimulator, while the regions, right under the copper wire where the current flows on the two sides of stimulator, also produce relatively high field intensity but with the opposite

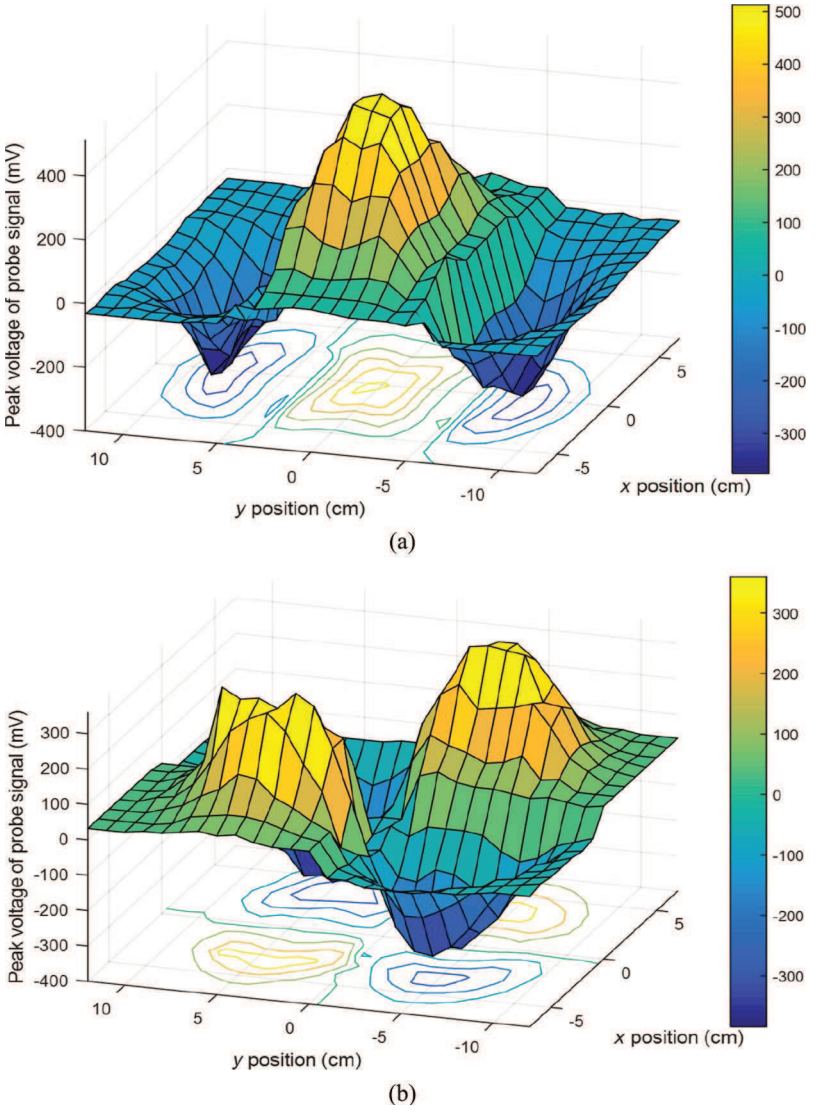

Figure 6. Three-dimensional plots of measurements of induced electric field x and y component amplitudes. (a) x component amplitude distribution plot, (b) y component amplitude distribution plot.

polarity. The *y* component of induced electric field shows a totally different distribution. Field detected by the probe at the figure-8 center was close to zero, while higher outputs were detected at the four corners of the figure-8

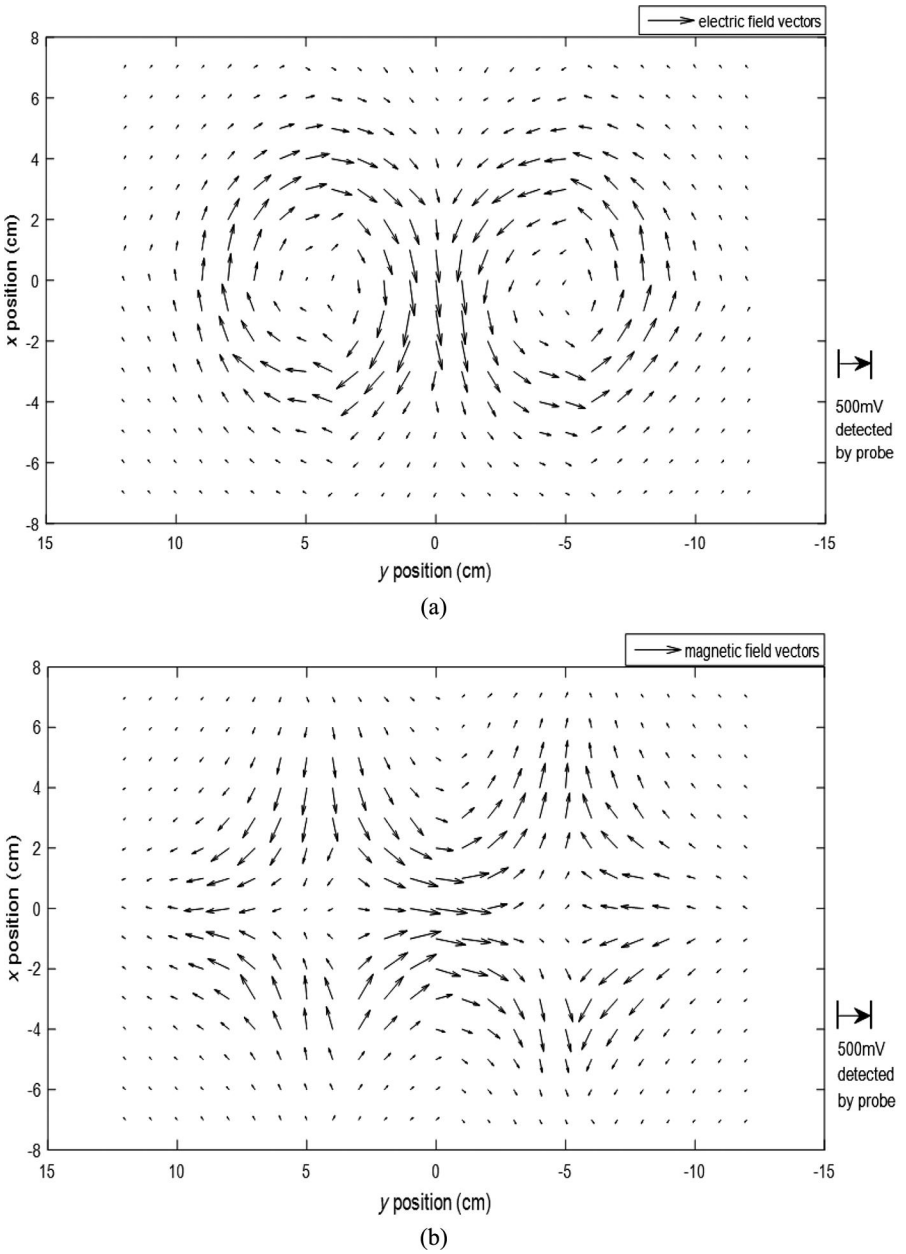

Figure 7. (a) Induced electric field distributions within plane $z = 0$; (b) magnetic field distribution within plane $z = 0$; (c) induced electric field distributions within plane $z = -2$; and (d) magnetic field distribution within plane $z = -2$. Field vectors' length represents the voltage detected by the probe at the corresponding position. Both types of probes can be calibrated with commercial TMS to convert voltage into field intensity. *Note*: TMS, Transcranial magnetic stimulation.

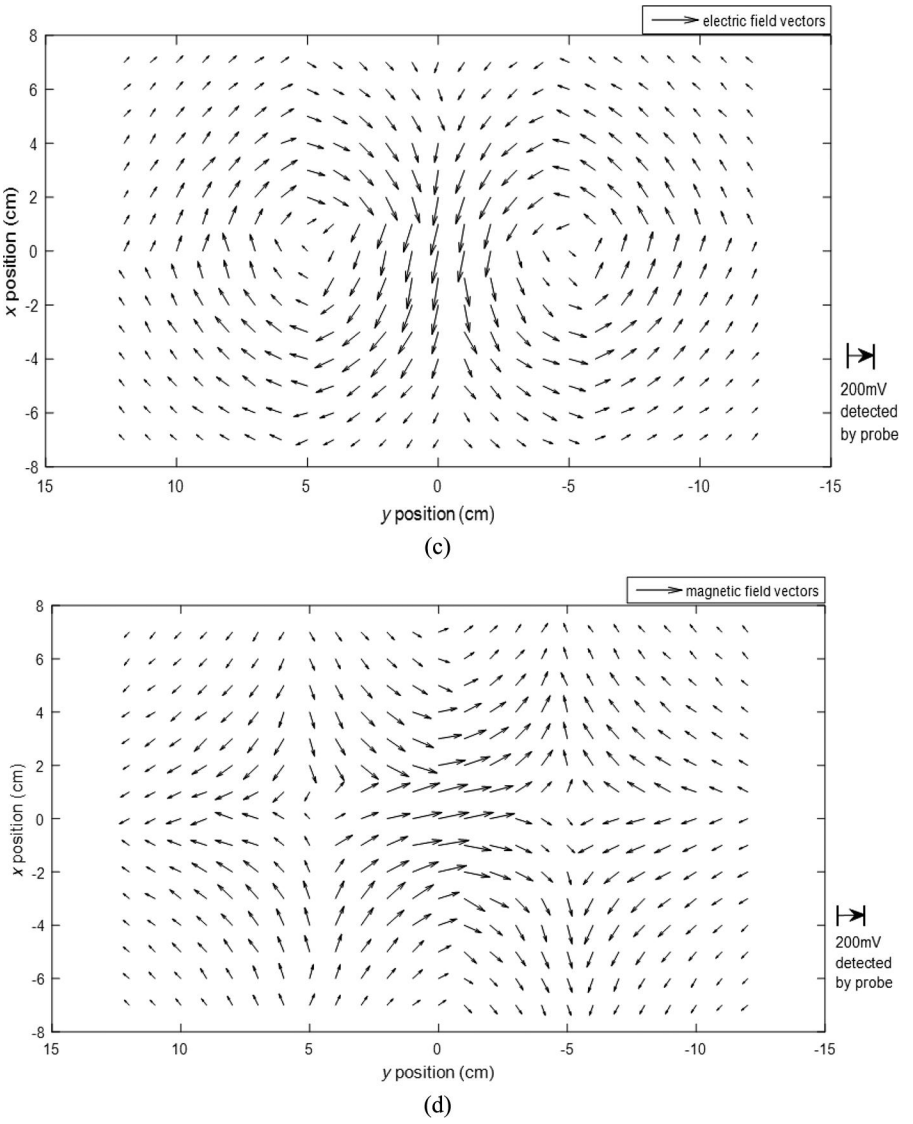

Figure 7. Continued.

region (still right under the copper wire where the current flows), and their polarity provides a diagonal feature. By combining x and y components, we can plot two-dimensional electric field vector distributions with MATLAB. Plots of induced electric field distribution in the $z = 0$ and $z = -2$ planes are presented in Figure 7a–c, while Figure 7b–d presents their corresponding two-dimensional magnetic field vector distribution. The E-field vector distribution closely follows the current flow in the stimulator. The closer to the copper wire, like $z = 0$, the higher the intensity of induced electric field. As the distance, z, increased, the length, representing the strength, of field vectors

tends to become uniformly distributed, which indicates that intensity of induced electric field was becoming weaker in the region further away from stimulator surface.

For direct electric filed measurement, we used the probe as shown in Figure 1b. We have used it to directly conduct a two-dimensional measurement, on the plane of $z = 0$ for both types of coils. By keeping all the other experiment setups and parameters the same, we measured both x and y components of the electric field vector. As shown in Figure 8, the measured electric field vector distribution of figure-8 coil was well matched with that measured with magnetic probe as shown in Figure 7a. We demonstrated that the induced electric field can be detected by both electric field and magnetic field probes. The former can directly measure electric field and the latter can detect the time derivative of magnetic field and then convert the measured data to induced electric field using Equations (3) and (4). To further verify this probe's capability of induced electric field sensing, we also used it to scan the area of $x < 0$ on $z = 0$ plane for the circular coil. Both electric field intensity plot and vector field plot in Figure 9 can match with theoretical plots.[10] The ring-shaped outline is clearly illustrated in the electric field intensity distribution. So this study experimentally demonstrated that our electric field probe can be used as an electric field sensor, not limited to current measurement only. With the minimization of probe size using small magnetic core, we can improve spatial resolution and at the same time obtain improved sensitivity and directivity.

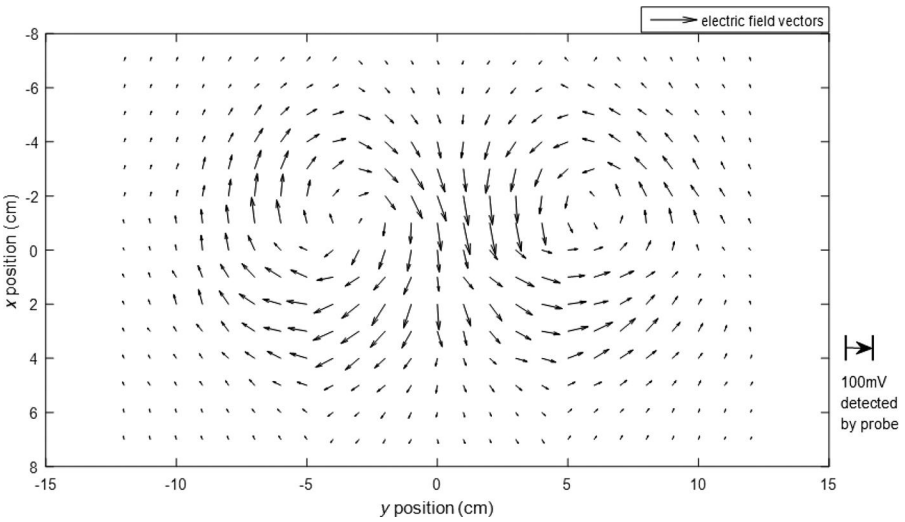

Figure 8. Two-dimensional projection on XY plane ($z = 0$) of induced electric field vectors measured by electric field probe.

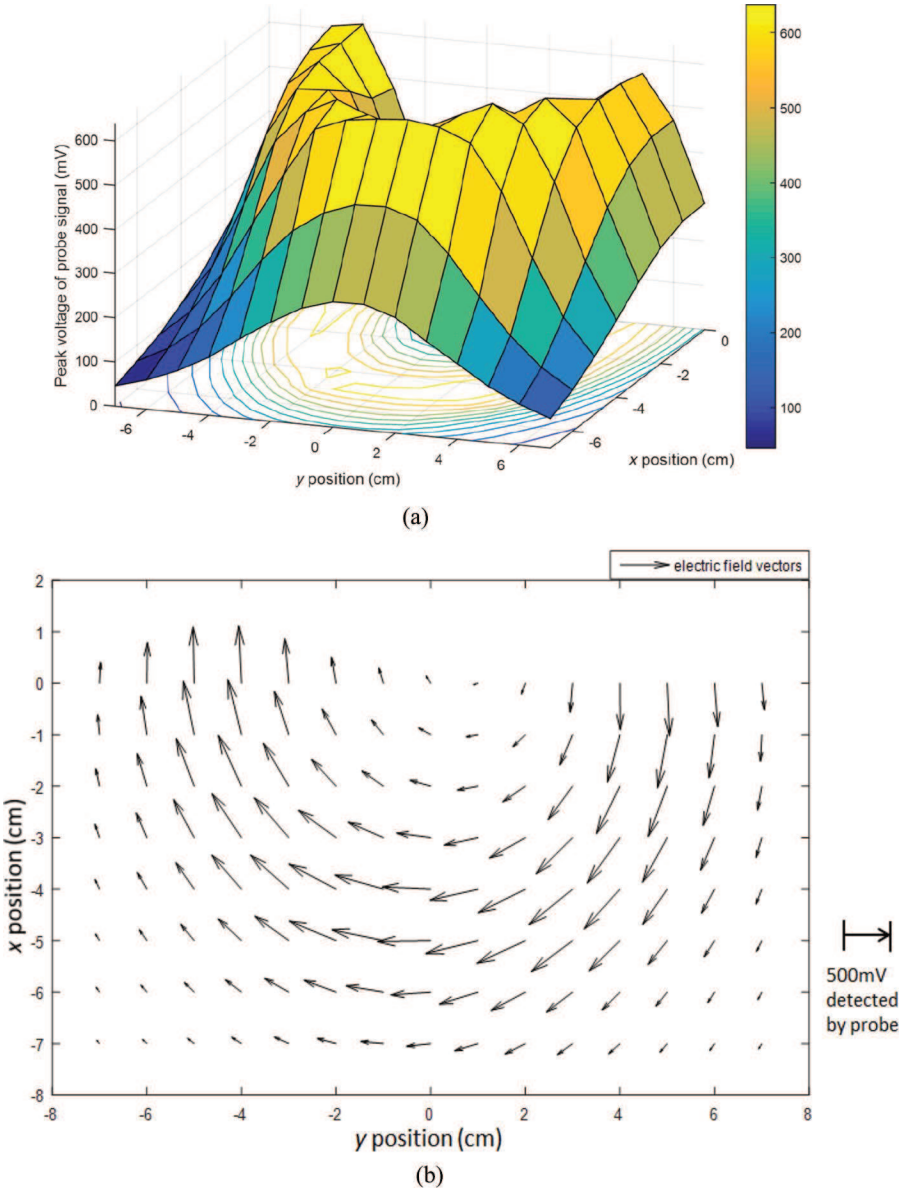

Figure 9. (a) Induced electric field intensity distribution of circular coil measured by electric field probe and (b) induced electric field vector plot of circular coil measured by electric field probe. Both measurements were completed within $x < 0$ area of $z = 0$ plane.

Transient field measurement in the brain phantom

According to Equations (1) and (8), induced electric field measurements in the brain phantom could be different from that in the air, since the current density term in Ampere's law was not zero in this case. However, the electric

displacement-changing rate generated by TMS dominated on the right side of this equation due to sharp increasing curve of voltage on the stimulator.

To demonstrate this, we compared both types of probes (including electric field probe and cylindrical inductor probe) to measure the field at one certain position in the air and artificial cerebrospinal fluid (ACSF-Ecocyte Bioscience, salinity ~0.9%) using the animal TMS as shown in Figure 3. The voltage that charged the capacitor C1 was set to 500 V. As Figure 10 illustrates, by comparing signals detected in each case, no significant difference between the measurements in the air and cerebrospinal fluid (CSF) liquid was observed for neither type of probe. The electric field probe detected a peak of 1200 mV in the air and 1240 mV in CSF liquid, only a 3.3% increase; and for the cylindrical inductor probe, the reading is 10.2 V in the air and 11.1 V in CSF. The 8.8% increase of peak voltage reading is attributed from

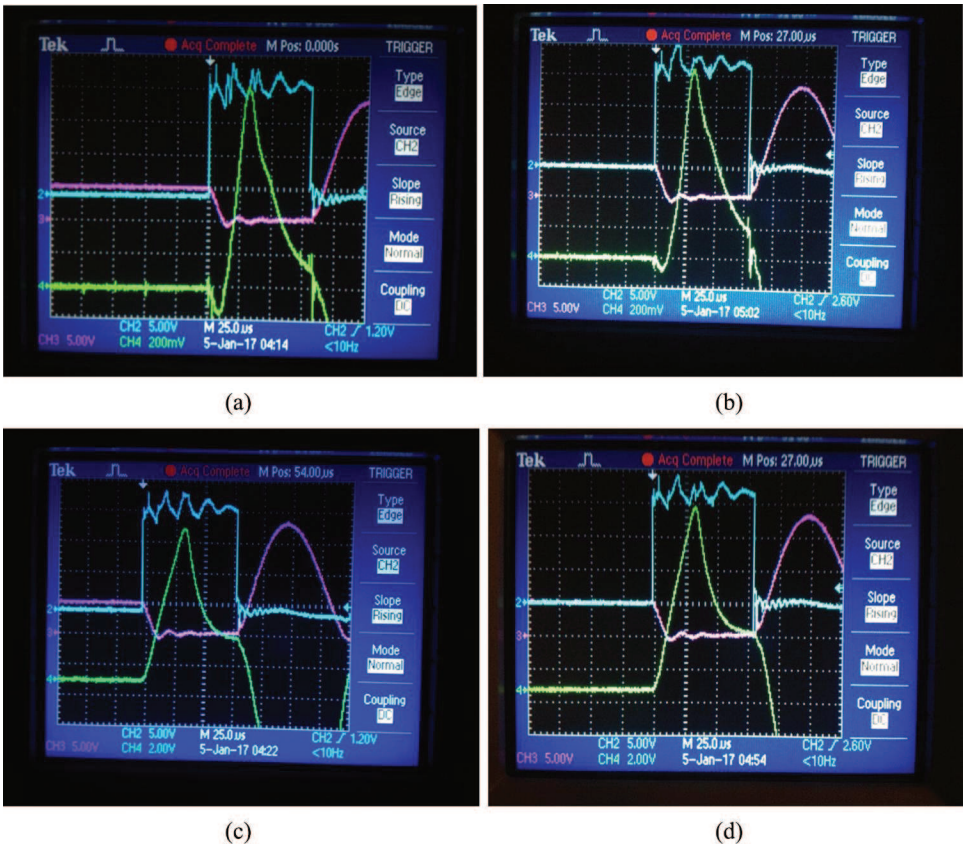

Figure 10. Comparison of field measurements in (a) salt water and (b) air using three types of probes. Signal detected by electric field probe in (c) salt water and (d) air. Signal detected by cylindrical inductor probe in salt water and in the air. For all oscilloscope screenshots, blue traces are the pulse on the IGBT gate; purple traces are the voltage curves on the IGBT collector and emitter and green traces present signals detected by probes. *Note*: IGBT, insulated gate bipolar transistor.

Table 1. Comparison of our probe, dipole probe, and silicon-on-chip sensor in electric field measurement.

Electric field probe type	Advantage(s)	Disadvantage(s)
Proposed probe	a. High sensitivity and no amplifier needed to amplify signal. b. Sensing signal is clean and with very low noise. c. High dynamic range from low to high field. d. Size of the probe is small. e. Fabrication of the probe is simple and low cost.	a. To display electric field signal, integrator circuit is needed to convert raw signal detected by the probe.
Dipole probe	a. Size of the probe can be small. b. Fabrication of the probe is simple and low cost.	a. Sensitivity of the probe is very low and always needs amplifier to make the signal visible on oscilloscope. b. Feed line of the probe can easily pick up electric signals from surrounding environment, so the signal is not clean and very noisy.
Silicon-on-chip electric field sensor	a. The probe size can be minimized to achieve the best spatial resolution.	a. Relatively low sensitivity. b. Higher cost due to microfabrication, packaging processes of the device. c. Some may have very limited measurement range.

the induced current in CSF. Comparison of three types of probes for electric field measurement is listed in Table 1, and it may require more detailed dynamic analysis including the driving current source generated from the capacitor bank, through the TMS coil, CSF conductance, and probe inductance, which will be done in future research.

Conclusion

Transient magnetic and electric field probes are important for developing future deep and focused TMS tools. In this study, we compared two types of probes that can measure field changes with high spatial resolution. We found that both of them are directional with polarity and can do *x*, *y*, *z* three-dimensional vector field measurements. The inductor type of magnetic probes and the electric field probes modified from Rogowski coil structure can equivalently measure two-dimensional electric field through Maxwell equations and mathematic conversion with high sensitivity. Measurements of field using these two types of probes did not show significant difference in the air and in CSF-filled brain phantom due to the relatively low eddy current in phantom compared with the electric displacement-changing rate and their low sensitivity to current density. As a result, the field distribution detected by these two types of probes can estimate field in brain tissues as well. However, the electric field probe has to be used to obtain three-dimensional induced electric field measurements. The magnetic field probe size can be further reduced and achieve very high-spatial resolution probes in the air. Using a

combination of these probes together, we can monitor and well calibrate new types of TMS systems in vector form and with very high spatial resolution.

ORCID

Qinglei Meng http://orcid.org/0000-0002-5173-3007

References

[1] Vaynman, S.; Gomez-Pinilla, F. Revenge of the "Sit": How Lifestyle Impacts Neuronal and Cognitive Health Through Molecular Systems that Interface Energy Metabolism with Neuronal Plasticity. *J. Neurosci. Res.* **2006**, *84*, 699–715.
[2] Pascual-Leone, A. Repetitive Transcranial Magnetic Stimulation: Technical Principles, Safety, and Potential Therapeutic Applications. *Electroen. Clin. Neuro.* **1997**, *103*, 48–49.
[3] Roth, B. J.; Peter, J. B. A Model of the Stimulation of a Nerve Fiber by Electromagnetic Induction. *IEEE Trans. Biomed. Eng.* **1990**, *37*, 588–597.
[4] Glover, P. M.; Bowtell, R. Measurement of Electric Fields due to Time-Varying Magnetic Field Gradients using Dipole Probes. *Phys. Med. Biol.* **2007**, *52*, 5119–5130.
[5] Lang, J.; Sances, A.; Larson, S. J. Determination of Specific Cerebral Impedance and Cerebral Current Density During Application of Diffuse Electrical Currents. *Med. Biol. Eng.* **1969**, *7*, 517–525.
[6] Jarzembski, W. B.; Larson, S. J.; Sances, A. Evaluation of Specific Cerebral Impedance and Cerebral Current Density. *Ann. NY Acad. Sci.* **1970**, *170*, 476–490.
[7] Swiontek, T. J.; Sances, A.; Larson, S. J.; Ackmann, J. J.; Cusick, J. F.; Meyer, G. A.; Miller, E. A. Spinal-Cord Implant Studies. *IEEE Trans. Biomed. Eng.* **1976**, *23*, 307–312.
[8] Hart, F. X.; Wood, K. W. Eddy Current Distributions-Their Calculation with a Spreadsheet and their Measurement with a Dual Dipole Antenna Probe. *Am. J. Phys.* **1991**, *59*, 461–467.
[9] Salinas, F. S.; Lancaster, J. L.; Fox, P. T. 3D Modeling of the Total Electric Field Induced by Transcranial Magnetic Stimulation using the Boundary Element Method. *Phys. Med. Biol.* **2009**, *54*, 3631–3647.
[10] Salinas, F. S.; Lancaster, J. L.; Fox, P. T. Detailed 3D Models of the Induced Electric Field of Transcranial Magnetic Stimulatoin Coils. *Phys. Med. Biol.* **2007**, *52*, 2879–2892.
[11] Lin, C.-Y.; Wang, A. X.; Lee, B. S.; Zhang, X.; Chen, R. T. High Dynamic Range Electric Field Sensor for Electromagnetic Pulse Detection. *Opt. Express.* **2011**, *19*, 17372–17377.
[12] Dolde, F.; Fedder, H.; Doherty, M. W.; Nobauer, T.; Rempp, F.; Balasubramanian, G; Wolf, T.; Reinhard, F.; Hollenberg, L. C. L.; Jelezko, F.; et al. Eletric-Field Sensing using Single Diamond Spins. *Nat. Phys.* **2011**, *7*, 459–463.
[13] Densmore, A.; Xu, D.-X.; Waldron, P.; Janz, S.; Cheben, P.; Lapointe, J.; Delage, A.; Lamontagne, B.; Schmid, J. H.; Post, E. A silicon-on-Insulator Photonic Wire Based Evanescent Field Sensor. *IEEE. Photon. Tech. Le.* **2006**, *23*, 2520–2522.
[14] Zeng, R.; Zhang, Y.; Chen, W.; Zhang, B. Measurement of Electric Field Distribution along Composite Insulators by Integrated Optical Electric Field Sensor. *IEEE. Trans. Dielect. El. In.* **2008**, *15*, 302–310.
[15] Shinagawa, M.; Fukumoto, M.; Ochiai, K.; Kyuragi, H. A Near-Field-Sensing Transceiver for Intrabody Communication Based on the Electrooptic Effect. *IEEE. Trans. Instrum. Meas.* **2004**, *53*, 1533–1538.